Published in final edited form as:
J Mol Cell Cardiol. 2013 May ; 58: 59–66. doi:10.1016/j.yjmcc.2013.01.002.

Calcium Movements Inside the Sarcoplasmic Reticulum of Cardiac Myocytes

Donald M. Bers[1] and **Thomas R. Shannon**[2]

[1]Department of Pharmacology, University of California, Davis, Davis, CA

[2]Department of Physiology and Biophysics, Rush University Chicago, IL

Abstract

Sarcoplasmic reticulum (SR) Ca content ($[Ca]_{SRT}$) is critical to both normal cardiac function and electrophysiology, and changes associated with pathology contribute to systolic and diastolic dysfunction and arrhythmias. The intra-SR free [Ca] ($[Ca]_{SR}$) dictates the $[Ca]_{SRT}$, the driving force for Ca release and regulates release channel gating. We discuss measurement of $[Ca]_{SR}$ and $[Ca]_{SRT}$, how $[Ca]_{SR}$ regulates activation and termination of release, and how Ca diffuses within the SR and influences SR Ca release during excitation-contraction coupling, Ca sparks and Ca waves. The entire SR network is connected and its lumen is also continuous with the nuclear envelope. Rapid Ca diffusion within the SR could stabilize and balance local $[Ca]_{SR}$ within the myocyte, but restrictions to diffusion can create spatial inhomogeneities. Experimental measurements and mathematical models of $[Ca]_{SR}$ to date have greatly enriched our understanding of these $[Ca]_{SR}$ dynamics, but controversies exist and may stimulate new measurements and analysis.

Keywords

sarcoplasmic reticulum; cardiac myocytes; calcium; ryanodine receptor; SR Ca release

1. Introduction

During cardiac E-C coupling (ECC) sarcolemmal depolarization leads to opening of L-type Ca channels, (LTCC) and Ca current (I_{Ca}) which initiates Ca-induced Ca release from the sarcoplasmic reticulum (SR) via ryanodine receptor (RyR) channels. Both channels are localized to specialized junctions between the plasma membrane and SR that are mostly in transverse- or T-tubules, although some junctions are also at the cell edge. The free [Ca] within the SR ($[Ca]_{SR}$) is very important because it dictates A) the driving force for SR Ca release, B) the amount of Ca bound to calsequestrin (CSQ) which is localized in junctional SR (JSR), and as such contributes to the total amount of SR Ca ($[Ca]_{SRT}$), and C) gating of the RyR, with respect to both activation and termination of SR Ca release.

Address for Correspondence: Donald M. Bers, Ph.D., Department of Pharmacology, University of California, Davis, 451 Health Sciences Drive, Davis, CA 95616, Phone: (530) 752-3200, FAX: (530) 752-7710, dmbers@ucdavis.edu.

Disclosures Nothing to declare.

2. Measuring $[Ca]_{SRT}$ and $[Ca]_{SR}$ and their effect on SR Ca release

The $[Ca]_{SRT}$ (typically ~120 μmol/l cytosol) is routinely measured by a rapidly evoked caffeine-induced Ca transient [1–4], and can be inferred by either the amplitude of the cytosolic Ca transient ($\Delta[Ca]_i$, ideally including correction for cytosolic Ca buffering) or by integration of the Na/Ca exchange (NCX) current (I_{NCX}) produced as released Ca is extruded from the cell (ideally correcting for parallel NCX-independent fluxes). For direct free $[Ca]_{SR}$ measurement in ventricular myocytes we use the low affinity fluorescent Ca indicator Fluo-5N (K_d=400 μM) that has very low basal fluorescence [5,6]. Thus only regions where [Ca] > 100 μM are visible (SR and nuclear envelope). This approach allows on-line real-time $[Ca]_{SR}$ measurement, but is not as simple to use in species other than rabbit (which we suspect is related to intra-SR esterase effectiveness). Combining measurement of $[Ca]_{SRT}$ and $[Ca]_{SR}$) in myocytes simultaneously allows direct measure of intra-SR Ca buffering characteristics [6]. During diastole about half of the $[Ca]_{SRT}$ is bound to CSQ or other intra-SR buffers (with low apparent affinity K_d ~ 600 μM).

Increasing $[Ca]_{SR}$ influences SR Ca release during ECC in a highly non-linear manner, with respect to both the amount of Ca released by a given I_{Ca} trigger and the fraction of the total SR Ca released [7–13]. At modest $[Ca]_{SR}$ and $[Ca]_{SRT}$ (~40% of the normal levels) SR Ca release cannot be triggered by normal I_{Ca}, but as $[Ca]_{SRT}$ increases, the fractional SR Ca release increases very steeply. Diastolic SR Ca leak, the frequency of Ca sparks and RyR2 open probability also have a similar $[Ca]_{SR}$-dependence [14–19]. This probably creates an upper limit to $[Ca]_{SR}$ which is below the thermodynamically limiting $[Ca]_{SR}$ that one might expect from the function of the SR Ca-ATPase [20]. A practical consequence of this for ECC is that a modest increase in cellular and SR Ca load can result in large increases in Ca release and contractility, but that when $[Ca]_{SR}$ decreases (as in heart failure) there is a tendency for Ca transients and contractility to be depressed. Another consequence of this relationship is that when $[Ca]_{SR}$ is high there is an increased propensity for diastolic SR Ca release in the form of Ca waves (especially when the RyR is sensitized) and these can cause delayed afterdepolarizations and triggered arrhythmias.

Ca-induced Ca-release during both ECC and spontaneous Ca sparks is inherently positive feedback and as such might be expected to release all of the SR Ca. However, we know that SR Ca release terminates for both ECC and Ca sparks at $[Ca]_{SR}$ approximately 0.4 mM or 40–50% of the normal $[Ca]_{SRT}$ [5,8,13,21–25]. Two possible explanations are that either the decline in local $[Ca]_{SR}$ contributes dynamically to the shut-off of RyR or that local $[Ca]_{SR}$ near the luminal mouth of the channel drops so low that $[Ca]_i$ in the junctional cleft also falls below the level required to maintain Ca-induced Ca-release. There is experimental evidence from several sources (including some of the above and RyR gating in lipid bilayers; [16,26,27]) supporting the idea that $[Ca]_{SR}$ dynamically participates in termination of SR Ca release (well before $[Ca]_{SR}$ approaches cytosolic levels). However, there is some data and computational modeling that emphasize that intra-SR diffusion is very highly restricted where the JSR meets the network or free SR (FSR) such that the $[Ca]_{SR}$ in the JSR can be nearly fully depleted (about half of $[Ca]_{SRT}$) without substantial depletion of the FSR [22,28]. Of course these explanations are not mutually exclusive and could coexist.

Several factors influence us to think the dynamic influence of local $[Ca]_{SR}$ on RyR gating may be the more important mechanism. First, the $[Ca]_{SR}$ at which SR Ca release terminates (~0.4 mM/ ~50% of normal $[Ca]_{SRT}$) coincides with both the SR Ca level at which I_{Ca} cannot trigger SR Ca release (i.e. ECC fails) [8,13] and the $[Ca]_{SR}$ at which spontaneous Ca sparks stop occurring (but would be detectable; [19]). This suggests that this $[Ca]_{SR}$ level (although malleable) exerts a powerful influence on RyR gating. Second, Ca blinks ($[Ca]_{SR}$ depletions associated with Ca sparks) terminate at the same $[Ca]_{SR}$ regardless of the rate of

release (and thus cleft $[Ca]_i$) at which that level is reached [19]. This suggests that local $[Ca]_{SR}$ might be a more important regulator of RyR gating in this situation than is cleft $[Ca]_i$, albeit the importance of cleft $[Ca]_i$ on RyR gating is indisputable. A third point regarding measurements of intra-SR gradients between JSR and FSR during ECC and Ca blinks requires consideration of Ca diffusion within the SR and will be discussed below [5,25,29,30].

3. Sarcomeric SR Structure

The SR structure in mammalian ventricular myocytes (Fig 1) has been measured by electron microscopy (EM), mostly done long ago [31,32] summarized in [1]. Both the volume and surface area of FSR are roughly ten times greater than of JSR, and the FSR network forms a mesh that surrounds the myofibrils (and mitochondria). Scanning EM images suggest broad swaths of FSR in a richly branched network that crosses sarcomere boundaries (both in series and parallel to their length; [33,34]). That approach might overestimate the FSR diameter vs. some classical and more recent EM work, but suggests an extensively connected SR network. More recent EM studies [22] described the JSR as thin (30 nm) pancake-like cisternae of diameter 590 nm wrapped around T-tubules that are filled with electron dense material (presumably CSQ) with on average 4.3 connections to the FSR network. Those authors suggested that this geometry might restrict diffusion between FSR and JSR, but at that time intra-SR diffusion had not been measured functionally. Fast Ca diffusion would limit spatial $[Ca]_{SR}$ gradients leading to more uniform release throughout the cell. On the other hand, slower diffusion could lead to spatial inhomogeneities with some regions having higher $[Ca]_{SR}$ either initially or during SR Ca release.

4. Measuring Diffusion of Ca and Fluo-5N inside SR

Wu and Bers [35] used intact myocytes with Fluo-5N loaded in the SR to directly assess diffusion of both Fluo-5N and Ca inside the SR. Fluorescence recovery after photobleach (FRAP) of Fluo-5N on one end of the myocyte allowed assessment of diffusion of the indicator inside the SR. This showed that the entire SR network and nuclear envelope throughout the myocyte are part of a single continuous compartment. That is, the lumen of the SR at any point is connected to the lumen everywhere else, without contents crossing a membrane. Moreover, the space within the nuclear envelope (between inner and outer nuclear membranes) is also contiguous with the SR network, and at rest the [Ca] there is the same as $[Ca]_{SR}$. These FRAP studies estimated the apparent diffusion coefficient for Fluo-5N (D^{SR}_{Fluo}) to be 8 $\mu m^2 s^{-1}$ using a simple 1-dimensional diffusion model. Picht *et al.* [25] extended this Fluo-5N FRAP analysis to compare longitudinal vs. transverse intra-SR diffusion of Fluo-5N, finding faster diffusion in the longitudinal vs. transverse direction (τ_{fast} = 1.56 ± 0.2 vs. 2.24 ± 0.2 s). This contrasted to the cytosolic diffusion of calcein, which was symmetrical in the longitudinal vs. transverse direction. Furthermore, correction for molecular weight differences of these fluorescent probes suggests that intra-SR diffusion is 3–times slower than cytosolic diffusion. While that difference could be influenced by several factors (e.g. binding of Fluo-5N or calcein to SR or cytosolic components) it might simply reflect the higher relative tortuosity of diffusion inside the SR vs. the cytosol.

Wu & Bers [35] also directly assessed Ca diffusion inside the SR, using a functionally analogous protocol to FRAP. Special conditions were set up where the SR Ca-ATPase was completely inhibited by thapsigargin, but $[Ca]_{SR}$ measured in a 90 s time window when the moderate $[Ca]_{SR}$ was well maintained. One end of the myocyte only was exposed very briefly to 10 mM caffeine to deplete local $[Ca]_{SR}$, and the recovery of local $[Ca]_{SR}$ was monitored (Fig 2). While the total $[Ca]_{SR}$ signal did not change during this recovery, $[Ca]_{SR}$ at the Ca-depleted end rose and at the other end $[Ca]_{SR}$ declined with a similar time

constant. Notably, the nuclear envelope at the left end of the cell recovered with a similar tau as the nearby SR. Similar diffusional modeling as used for Fluo-5N gave an estimate of the intra-SR apparent Ca diffusion coefficient D_{Ca}^{SR} of 60 $\mu m^2/s$. This is 7.5 times faster than the D_{Fluo}^{SR}, which agrees well with the expected factor of 5.3 based on molecular weight differences. This D_{Ca}^{SR} is roughly 10 times slower than in free aqueous solution, but still seems relatively fast. Factors responsible for slowing D_{Ca}^{SR} might include Ca binding to fixed buffers and high viscosity or path tortuosity inside the SR. Since one might expect binding of Ca and Fluo-5N to fixed buffers to differ but path tortuosity to be the same, tortuosity of the SR network might be the major cause of the slowing of the measured D_{Ca}^{SR} (and D_{Fluo}^{SR}) vs. that expected in aqueous solution. The presence of known fixed Ca buffers (e.g. CSQ) would tend to slow the estimated D_{Ca}^{SR}, but since these are low affinity sites with rapid off-rates, this effect may be small. Based on the factor $(1+(K_d+[B_{max}])/(K_d[Ca])^2$; [36]) the measured D_{Ca}^{SR} could be ~3 times smaller than the actual value (for K_d, B_{max} and $[Ca]_{SR}$ of 0.6, 2 and 1 mM, respectively). The presence of diffusible buffer in the SR (50–100 μM Fluo-5N) would facilitate diffusion, but not appreciably alter D_{Ca}^{SR} [29].

Swietach *et al.* [29] used a clever indirect approach to estimate D_{Ca}^{SR} in ventricular myocytes using $[Ca]_i$ during pairs of caffeine-induced Ca transients (again with the SR Ca-ATPase blocked). The first caffeine was restricted to one end of the cell to deplete $[Ca]_{SRT}$ there (analogous to the Wu & Bers study). The second caffeine was global to assess by regional $[Ca]_i$ amplitude how well the depleted SR region had recovered. Using a computational model they inferred a relatively slow D_{Ca}^{SR} value (8–9 $\mu m^2/s$). They showed that if they had ignored the leak-dependent $[Ca]_{SRT}$ decline which was evident in their experiments their model D_{Ca}^{SR} value would have been higher (~40 $\mu m/s^2$). They suggested that the Wu and Bers [35] D_{Ca}^{SR} estimate of 60 $\mu m/s^2$ might be due to an exact match of residual SERCA activity and SR Ca leak (despite evidence in that paper that both were negligible for the measurements). In any event, the model of Swietach *et al.* [29] suggests that very large JSR-FSR gradients of $[Ca]_{SR}$ are likely to occur during SR Ca release. This would be consistent with slow and restricted diffusion between JSR and FSR as suggested by Brochet *et al.* [22]. While the actual D_{Ca}^{SR} is not fully resolved, it is important to consider the functional impact it has on measured spatiotemporal gradients of $[Ca]_{SR}$ during SR Ca release.

5. Ca Scraps and Blinks: Spatiotemporal Properties

We first called these local $[Ca]_{SR}$ depletion Ca “scraps” [5] as an anagram-like homage to the term Ca “sparks” [14]. The first measurements of simultaneous Ca sparks and scraps [22] coined “Ca blinks” (for scraps during sparks) and we accept this refinement. They showed that Ca sparks peak before the blink nadir, and that suggests that release continues for some time after the Ca spark peak, perhaps at a reduced rate. Some of their Ca blinks were much smaller in amplitude and shorter in duration and recovery time constant (τ_{recov} ~29 ms) than Ca scraps seen during ECC (τ_{recov} ~150 ms). The rapid JSR refilling they attributed to rapid intra-SR diffusion compared to SR Ca uptake, but since they did not detect $[Ca]_{SR}$ depletion in the FSR during Ca blinks, they suggested that FSR-JSR diffusion is restricted. This apparent dichotomy required further work for clarification.

Zima *et al.* [24] analyzed Ca sparks and blinks recorded simultaneously in rabbit ventricular myocytes. Figure 3A shows that when compared to global Ca transients and Ca scraps, the amplitude and kinetics of the average Ca blinks and scraps are remarkably similar to one another (~0.5 $\Delta F/F_0$ and τ_{recov} ~150 ms; see also [37]). That contrasts with the $[Ca]_i$ signals

where Ca sparks are smaller in amplitude and much shorter in duration than Ca transients. This latter point is well known and the conventional wisdom (with which we agree) is that the global Ca transient is the spatiotemporal sum of individual Ca spark-like events that overlap in time and space. For Ca blinks there seems to be less spatiotemporal overlap. This would be consistent with the idea that each Ca blink obtains most of its Ca for release from its own "sphere of influence" and $[Ca]_{SR}$ depletion at one junction has little impact on $[Ca]_{SR}$ at the next junction. This sounds like relatively restricted Ca diffusion.

Zima *et al.* [24] also showed that there was a much higher variation in the τ_{recov} of blinks vs. sparks. Some blinks exhibited τ_{recov} as short as the 29 ms noted above, but some were as long as 500 ms (mean= 161 ms). Notably, the τ_{recov} variability was anatomical rather than stochastic, because there was extremely tight correlation (R^2=0.98) for τ_{recov} between additional Ca blinks occurring at the same site. We also showed that the combination of partial block of RyR conductance and elevation of $[Ca]_{SR}$ caused very long-lasting Ca sparks to occur (lasting > 1 s). We think that these occur because the local $[Ca]_{SR}$ at the active JSR can stay above the termination threshold when the flux rate is reduced. That is, the release flux rate can be maintained adequately by intra-SR diffusion to prevent local JSR $[Ca]_{SR}$ from getting too low. We mention this here, because it was shown that the JSR regions where these long events occur correlate with JSR regions which seem especially well connected (based on simultaneous FRAP measurements that assessed intra-SR Fluo-5N diffusion). So, it seems clear that there is large variability among JSR regions with respect to how well they are diffusionally connected to the rest of the SR network. That may also explain some of the variability of Ca blink kinetics reported in the literature.

In our initial Ca scraps paper [5] we were unable to detect a significant spatiotemporal $[Ca]_{SR}$ gradient during normal SR Ca release (see also Fig 3B). The implication was that Ca diffusion within the SR was fast enough that the whole SR network depleted in apparent unison. Of course, if the release is restricted to the JSR, there must be greater depletion around the mouths of the open RyR channels, but we were unable to detect it, in part because the small volume and point spread function [38]. We revisited this in 2011 [25] and found essentially the same thing (Fig 3B). There were two possible explanations, either diffusion is quite fast within the SR or we lack the resolution to detect it reliably (or both). So we also carefully studied spatiotemporal $[Ca]_{SR}$ gradients during Ca blinks, where by definition a $[Ca]_{SR}$ gradient must exist between the JSR unit producing the Ca blink and the rest of the regional SR which is not releasing Ca.

Ca blinks and sparks were measured in permeabilized myocytes (Fig 3C). As is evident in both plot profiles (middle) and x-t images (bottom), significant $[Ca]_{SR}$ gradients developed between the mid-sarcomere (0.8 μm, gray) and the junction (black). Both the gradients and the time to nadir relative to the junction increased with distance (Fig 3D). Interestingly, gradients were more significant when the Ca profile was measured transversally across the myocyte, indicating that diffusion may be more restricted in this direction on average. Grouping longitudinal data by the τ_{recov} of $[Ca]_{SR}$ in the JSR also led to the conclusion that those with fast recovery (and broader spatial depletion) were better connected to surrounding junctions than those with slower recovery. The nadir in these fast/connected JSR sites was also slightly shallower, again consistent with better $[Ca]_{SR}$ support from neighboring regions. This reiterates the above variable connectivity of individual junctions.

6. Mathematical Modeling of $[Ca]_{SR}$ during SR Ca release

Several groups recently modeled $[Ca]_{SR}$ gradients during release [25,28,29]. We used a half-sarcomere model to simulate SR Ca release where all JSRs release (Fig 4A) assuming the same behavior across each boundary (creating simple no-flux boundary conditions) [25].

That is, the horizontal half sarcomeres mirror these $[Ca]_{SR}$ changes across the Z- and M-line and the parallel sarcomeres exhibit parallel behavior. We accounted for all relevant fluxes (e.g. SR Ca uptake and release, CSQ in the JSR etc.) and used a pre-estabished Ca release waveform [13,25]. Figure 4B shows local $[Ca]_i$ and $[Ca]_{SR}$ at different distances from the JSR (with D_{Ca}^{SR}=60 μm^2/s) with an inset mimicking blurring for JSR and M-line (mean of 200 nm on either side). There was little difference in $[Ca]_{SR}$ waveform as seen experimentally [5,22,25]. Looking at the influence of D_{Ca}^{SR} on the difference in $[Ca]_{SR}$ depletion (FSR-JSR; Fig 4C), D_{Ca}^{SR} must be at least >30 μm/s^2 for the difference to be <20% and exhibit delays <20 ms. For D_{Ca}^{SR}=10 μm/s^2 we would expect a 38% difference in FSR vs. JSR depletion amplitude and a >60 ms delay in time to nadir that is not seen experimentally. So, is this fast D_{Ca}^{SR} of 60 μm/s^2 consistent with $[Ca]_{SR}$ gradients seen during Ca blinks?

For Ca blinks the model must be extended because one JSR release site might draw Ca from multiple sarcomeres in all directions. We used a grid of release units (Fig 5A) with two full sarcomeres in x, y and z directions (28 nearest JSRs, which sufficed; [25]). Now, of course there must be a $[Ca]_{SR}$ gradient because very far away $[Ca]_{SR}$ must be unperturbed. The ~40% difference in FSR vs. JSR seen experimentally (Fig 3C–D) is consistent with a broader range of D_{Ca}^{SR} than just 30–90 μm/s^2, but the extent of FSR depletion and short delay in nadir seen experimentally (10–20 ms) are most consistent with this range of D_{Ca}^{SR}. Using the same SR Ca release waveform for a blink produced smaller JSR depletion than during ECC. This raised the possibility that release during a blink may continue for longer, exactly because Ca diffusion from neighboring sarcomeres (unavailable during ECC) delays JSR $[Ca]_{SR}$ reaching the shut-off level. So we let release termination be driven by JSR $[Ca]_{SR}$ (release terminated exponentially at 40% depletion) and that allowed more realistic Ca blink amplitude and kinetics (Fig 6B).

Figure 6A–B shows that the model with D_{Ca}^{SR}=60 μm/s^2 reasonably recapitulates spatiotemporal characteristics observed experimentally, and much better than D_{Ca}^{SR}<10 μm/s^2. Moreover, we could simulate the variation in JSR connectivity simply by altering D_{Ca}^{SR} between 40 and 90 μm/s^2 (Fig 6C). A similar adjustment in transverse vs. longitudinal D_{Ca}^{SR} (faster longitudinally) could also explain the differences in spatiotemporal $[Ca]_{SR}$ gradient measured during Ca blinks experimentally [25].

An important aspect that emerged from our modeling analysis is that SR Ca release does not shut-off completely at the peak of the Ca transient or spark. As discussed above, this is also a direct conclusion from the delay between Ca spark peak and Ca blink nadir [22,24]. It also seems consistent with the appearance of sub-spark size SR Ca release events [19,39,40] that can occur under conditions where easily detectable Ca sparks are no longer seen. Thus, SR Ca release may rise quickly to a peak during ECC, but may continue at a very much lower (and declining) level during the cardiac action potential [25,41]. This may be, in fact, analogous to the rapid I_{Ca} inactivation during SR Ca release, but sustained very low level of I_{Ca} throughout the plateau phase of the action potential [42].

7. Intra SR Ca Diffusion can alter Wave Propagation

We traditionally think of Ca wave propagation as driven entirely by cytosolic Ca waves initiated by one JSR being sufficient to activate the next JSR via Ca-induced Ca-release, where elevated $[Ca]_{SR}$ and $[Ca]_i$ can facilitate wave occurrence. However, it is interesting to consider how intra-SR diffusion can influence wave propagation. The first study on this topic [43] suggested that blocking SR Ca-ATPase actually accelerated wave propagation.

That could occur because SR Ca uptake between JSR sites would limit how high $[Ca]_i$ is when the cytosolic wave hits the next JSR and that could reduce wave fidelity and propagation rate. This would also be an attractive explanation for why SERCA2 overexpression, as currently used in clinical trials [44] can be anti-arrhythmic rather than pro-arrhythmic as would be expected from the effects of SERCA enhancement to increase SR Ca loading and Ca spark initiation.

Somewhat opposite result have been obtained with SERCA inhibition by either adding the inhibitor into the bath [45] or by flash photolytic uncaging of SERCA inhibitor [46]. In both cases, SERCA block slowed rather than accelerated Ca wave propagation. O'Neill *et al.* [45] concluded this slowing was because of lower SR Ca content during their measurements. However, the more rapid SERCA block by Keller *et al.* [46] prevented SR Ca load change, and they still saw slower wave propagation. They concluded that fast SR uptake and intra-SR diffusion could facilitate wave propagation by loading SR ahead of the wave front. Direct $[Ca]_{SR}$ measurements [47] have shown that $[Ca]_{SR}$ can indeed rise ahead of an approaching Ca wave and this has been attributed to SR Ca uptake driven by high $[Ca]_i$ ahead of the wavefront. This is consistent with a modeling study [28] which suggested that SERCA could drive $[Ca]_{SR}$ above the diastolic level ahead of a wave and sensitize the next junction for $D_{Ca}^{SR} \leq 60\ \mu m/s^2$. Although some details need to be worked out with respect to the conditions, JSR regions and model parameters [48], this clearly demonstrates an important role for intra-SR Ca diffusion and gradients in the genesis and stability of Ca waves. One can well imagine that these effects coexist and that different SR Ca loading conditions or even different junctions (better or less well connected to the FSR) could cause opposite results. That is, for junctions that have very high connectivity (high D_{Ca}^{SR}) there might be $[Ca]_{SR}$ depletion ahead of the wave which would reduce propagation. In contrast, weakly connected junctions (that have much SERCA function) could boost $[Ca]_{SR}$ locally and that would enhance JSR sensitivity and enhance propagation.

8. Conclusions

The SR is unique amongst the major cardiac organelles in their elongated tortuous structure, with JSR coupled to plasma membrane Ca channel domains and containing fast, low affinity Ca buffering within the release unit. The SR Ca release is critical for the regulation of synchronous contraction and also in triggering arrhythmias. This makes characterizing Ca movements within the SR of particular importance, but also challenging.

Direct dynamic measurement of $[Ca]_{SR}$ with fluorescent indicators has opened up this field of inquiry. However, the experimental and modeling results still contain some controversy. Slow diffusion coefficient more easily describes large $[Ca]_{SR}$ gradients during Ca blinks. On the other hand, a faster diffusion coefficient more fully describes the data available and can still explain such $[Ca]_{SR}$ gradients. However, a continuing late phase of SR Ca release is relatively new consideration that may be important, but is also hard to measure directly. Furthermore, potential differences in species or disease conditions in cardiac myocytes have yet to be examined fully. While great headway has been made in recent years, more experiments and modeling will be needed to give us a full understanding of the dynamics and regulation of local $[Ca]_{SR}$ in cardiac myocytes.

Acknowledgments

Funding

Supported by NIH grants R37-HL030077, R01-HL92097 (DMB), R01-HL071893 (TRS).

Abbreviations

$[Ca]_i$	free cytosolic [Ca]
$[Ca]_{SR}$	free sarcoplasmic reticulum [Ca]
$[Ca]_{SRT}$	total sarcoplasmic reticulum [Ca]
$\Delta[Ca]_i$	cytosolic Ca transient
CSQ	calsequestrin
D_{Ca}^{SR}	apparent diffusion coefficient for Ca inside the SR
D_{Fluo}^{SR}	apparent diffusion coefficient for Fluo-5N inside the SR
ECC	excitation-contraction coupling
I_{Ca}	Ca current
I_{NCX}	Na/Ca exchange current
FSR	free sarcoplasmic reticulum
JSR	junctional sarcoplasmic reticulum
LTCC	L-type Ca channel
NCX	Na/Ca exchange
RyR	ryanodine receptor
SR	sarcoplasmic reticulum

References

1. Bers, DM. Exciation-Contraction Coupling and Cardiac Contractile Force. Dordrecht, Netherlands: Kluwer Academic Publ; 2001.
2. Trafford AW, Díaz ME, Eisner DA. A novel, rapid and reversible method to measure Ca buffering and time-course of total sarcoplasmic reticulum Ca content in cardiac ventricular myocytes. Pflugers Arch. 1999; 437:501–503. [PubMed: 9914410]
3. Bassani JW, Bassani RA, Bers DM. Ca^{2+} cycling between sarcoplasmic reticulum and mitochondria in rabbit cardiac myocytes. J Physiol. 1993; 460:603–621. [PubMed: 8387590]
4. Ginsburg KS, Bers DM. Modulation of excitation-contraction coupling by isoproterenol in cardiomyocytes with controlled SR Ca^{2+} load and Ca^{2+} current trigger. J Physiol. 2004; 556:463–480. [PubMed: 14724205]
5. Shannon TR, Guo T, Bers DM. Ca^{2+} scraps. local depletions of free [Ca^{2+}] in cardiac sarcoplasmic reticulum during contractions leave substantial Ca^{2+}reserve. Circ Res. 2003; 93:40–45. [PubMed: 12791706]
6. Guo T, Ai X, Shannon TR, Pogwizd SM, Bers DM. Intra-sarcoplasmic reticulum free [Ca] and buffering in arrhythmogenic failing rabbit heart. Circ Res. 2007; 101:802–810. [PubMed: 17704210]
7. Isenberg G, Han S. Gradation of Ca^{2+}-induced Ca^{2+} release by voltage-clamp pulse duration in potentiated guinea-pig ventricular myocytes. J Physiol. 1994; 480:423–438. [PubMed: 7869257]
8. Bassani JW, Yuan W, Bers DM. Fractional SR Ca release is regulated by trigger Ca and SR Ca content in cardiac myocytes. Am. J. Physiol. 1995; 268:C1313–C1319. [PubMed: 7762626]
9. Spencer CI, Berlin JR. Control of sarcoplasmic reticulum calcium release during calcium loading in isolated rat ventricular myocytes. J Physiol. 1995; 488:267–279. [PubMed: 8568669]
10. Dettbarn C, Palade P. Ca^{2+} feedback on “quantal” Ca^{2+} release involving ryanodine receptors. Mol. Pharmacol. 1997; 52:1124–1130. [PubMed: 9396782]

11. Hüser J, Bers DM, Blatter LA. Subcellular properties of [Ca^{2+}]i transients in phospholamban-deficient mouse ventricular cells. Am J Physiol. 1998; 274:H1800–H1811. [PubMed: 9612393]
12. Santana LF, Gómez AM, Kranias EG, Lederer WJ. Amount of calcium in the sarcoplasmic reticulum: influence on excitation-contraction coupling in heart muscle. Heart Vessels Suppl. 1997; 12:44–49.
13. Shannon TR, Ginsburg KS, Bers DM. Potentiation of fractional sarcoplasmic reticulum calcium release by total and free intra-sarcoplasmic reticulum calcium concentration. Biophys J. 2000; 78:334–343. [PubMed: 10620297]
14. Cheng H, Lederer WJ, Cannell MB. Calcium sparks: elementary events underlying excitation–contraction coupling in heart muscle. Science. 1993; 262:740–744. [PubMed: 8235594]
15. Satoh H, Blatter LA, Bers DM. Effects of $[Ca]_i$, Ca^{2+} load and rest on Ca^{2+} spark frequency in ventricular myocytes. Am. J. Physiol. 1997; 272:H657–H668. [PubMed: 9124422]
16. Györke I, Györke S. Regulation of the cardiac ryanodine receptor channel by luminal Ca^{2+} involves luminal Ca^{2+} sensing sites. Biophysical Journal. 1998; 75:2801–2810. [PubMed: 9826602]
17. Shannon TR, Ginsburg KS, Bers DM. Quantitative assessment of the SR Ca^{2+} leak-load relationship. Circ Res. 2002; 91:594–600. [PubMed: 12364387]
18. Santiago DJ, Curran JW, Bers DM, Lederer WJ, Stern MD, Ríos E, Shannon TR. Ca sparks do not explain all ryanodine receptor-mediated SR Ca leak in mouse ventricular myocytes. Biophys J. 2010; 98:2111–2120. [PubMed: 20483318]
19. Zima AV, Bovo E, Bers DM, Blatter LA. Ca^{2+} spark-dependent and -independent sarcoplasmic reticulum Ca^{2+} leak in normal and failing rabbit ventricular myocytes. J. Physiol. 2010; 588:4743–4757. [PubMed: 20962003]
20. Shannon TR, Bers DM. Assessment of intra-SR free [Ca] and buffering in rat heart. Biophys. J. 1997; 73:1524–1531. [PubMed: 9284319]
21. Stern MD, Cheng H. Putting out the fire: what terminates calcium-induced calcium release in cardiac muscle? Cell Calcium. 2004; 35:591–601. [PubMed: 15110149]
22. Brochet DX, Yang D, DiMaio A, Lederer WJ, Franzini-Armstrong C, Cheng H. Ca^{2+} blinks: rapid nanoscopic store calcium signaling. Proc Natl Acad Sci USA. 2005; 102:3099–3104. [PubMed: 15710901]
23. Terentyev D, Viatchenko-Karpinski S, Valdivia HH, Escobar AL, Györke S. Luminal Ca^{2+} controls termination and refractory behavior of Ca^{2+}-induced Ca^{2+} release in cardiac myocytes. Circ Res. 2002; 91:414–420. [PubMed: 12215490]
24. Zima AV, Picht E, Bers DM, Blatter LA. Termination of cardiac Ca^{2+} sparks: role of intra-SR [Ca^{2+}], release flux, and intra-SR Ca^{2+} diffusion. Circ Res. 2008; 103:e105–e115. [PubMed: 18787194]
25. Picht E, Zima AV, Shannon TR, Duncan AM, Blatter LA, Bers DM. Dynamic calcium movement inside cardiac sarcoplasmic reticulum during release. Circ Res. 2011; 108:847–856. [PubMed: 21311044]
26. Sitsapesan R, Williams AJ. Regulation of the gating of the sheep cardiac sarcoplasmic reticulum Ca^{2+}-release channel by luminal Ca^{2+} J Membr Biol. 1994; 137:215–226. [PubMed: 8182731]
27. Qin J, Valle G, Nani A, Nori A, Rizzi N, Priori SG, Volpe P, Fill M. Luminal Ca^{2+} Regulation of Single Cardiac Ryanodine Receptors: Insights Provided by Calsequestrin and Its Mutants. J Gen Physiol. 2008; 131:325–334. [PubMed: 18347081]
28. Ramay HR, Jafri MS, Lederer WJ, Sobie EA. Predicting local SR Ca^{2+} dynamics during Ca^{2+} wave propagation in ventricular myocytes. Biophys J. 2010; 98:2515–2523. [PubMed: 20513395]
29. Swietach P, Spitzer KW, Vaughan-Jones RD. Ca^{2+}-mobility in the sarcoplasmic reticulum of ventricular myocytes is low. Biophys. J. 2008; 95:1412–1427. [PubMed: 18390622]
30. Swietach P, Spitzer KW, Vaughan-Jones RD. Modeling calcium waves in cardiac myocytes: importance of calcium diffusion. Front Biosci. 2010; 15:661–680. [PubMed: 20036839]
31. Page E, Surdyk-Droske M. Distribution, surface density, and membrane area of diadic junctional contacts between plasma membrane and terminal cisterns in mammalian ventricle. Circ Res. 1979; 45:260–267. [PubMed: 376173]

32. Fawcett DW, McNutt NS. The ultrastructure of the cat myocardium. I. Ventricular papillary muscle. J Cell Biol. 1969; 42:1–45. [PubMed: 4891913]
33. Ogata T, Yamasaki Y. High-resolution scanning electron microscopic studies on the three-dimensional structure of the transverse-axial tubular system, sarcoplasmic reticulum and intercalated disc of the rat myocardium. Anat Rec. 1990; 228:277–287. [PubMed: 2260783]
34. Yamasaki Y, Furuya Y, Araki K, Matsuura K, Kobayashi M, Ogata T. Ultra-high-resolution scanning electron microscopy of the sarcoplasmic reticulum of the rat atrial myocardial cells. Anat Rec. 1997; 248:70–75. [PubMed: 9143669]
35. Wu X, Bers DM. Sarcoplasmic reticulum and nuclear envelope are one highly interconnected Ca^{2+} store throughout cardiac myocyte. Circ Res. 2006; 99:283–291. [PubMed: 16794184]
36. Wagner J, Keizer J. Effects of rapid buffers on Ca^{2+} diffusion and Ca^{2+} oscillations. Biophys J. 1994; 67:447–456. [PubMed: 7919018]
37. Terentyev D, Kubalova Z, Valle G, Nori A, Vedamoorthyrao S, Terentyeva R, Viatchenko-Karpinski S, Bers DM, Williams SC, Volpe P, Gyorke S. Modulation of SR Ca release by luminal Ca and calsequestrin in cardiac myocytes: effects of CASQ2 mutations linked to sudden cardiac death. Biophys J. 2008; 95:2037–2048. [PubMed: 18469084]
38. Hake J, Edwards AG, Yu Z, Kekenes-Huskey PM, Michailova AP, McCammon JA, Holst MJ, Hoshijima M, McCulloch AD. Modelling cardiac calcium sparks in a three-dimensional reconstruction of a calcium release unit. J Physiol. 2012; 590:4403–4422. [PubMed: 22495592]
39. Brochet DX, Xie W, Yang D, Cheng H, Lederer WJ. Quarky calcium release in the heart. Circ Res. 2011; 108:210–218. [PubMed: 21148431]
40. Sato D, Bers DM. How does stochastic ryanodine receptor-mediated Ca Leak fail to initiate a Ca Spark? Biophys J. 2011; 101:2370–2379. [PubMed: 22098735]
41. Sobie EA, Dilly KW, Dos Santos CJ, Lederer WJ, Jafri MS. Termination of cardiac Ca^{2+} sparks: an investigative mathematical model of calcium-induced calcium release. Biophysicale. J. 2002; 83:59–78.
42. Morotti S, Grandi E, Summa A, Ginsburg KS, Bers DM. Improved L-type Ca^{2+} current and sarcoplasmic reticulum Ca^{2+}release models in rabbit ventricular excitation-contraction coupling. J Physiol. 2012; 590:4465–4481. [PubMed: 22586219]
43. Lukyanenko V, Subramanian S, Gyorke I, Wiesner TF, Gyorke S. The role of luminal Ca^{2+} in the generation of Ca^{2+} waves in rat ventricular myocytes. J Physiol. 1999; 518:173–186. [PubMed: 10373699]
44. Cutler MJ, Wan X, Plummer BN, Liu H, Deschenes I, Laurita KR, Hajjar RJ, Rosenbaum DS. Targeted SERCA2a gene delivery to restore electrical stability in the failing heart. Circulation. 2012 (In Press).
45. O'Neill SC, Miller L, Hinch R, Eisner DA. Interplay between SERCA and sarcolemmal Ca2+ efflux pathways controls spontaneous release of Ca2+ from the sarcoplasmic reticulum in rat ventricular myocytes. J Physiol. 2004; 559:121–128. [PubMed: 15194743]
46. Keller M, Kao JPY, Egger M, Niggli E. Calcium waves driven by “sensitization” wave-fronts. Cardiovasc. Res. 2007; 74:39–45. [PubMed: 17336953]
47. Maxwell JT, Blatter LA. Facilitation of Cytosolic Calcium Wave Propagation by Local Calcium Uptake into the Sarcoplasmic Reticulum in Cardiac Myocytes. J Physiol. 2012 (In Press).
48. Sobie EA, Lederer WJ. Dynamic local changes in sarcoplasmic reticulum calcium: physiological and pathophysiological roles. J Mol Cell Cardiol. 2012; 52:304–311. [PubMed: 21767546]

Highlights

- Cardiac intra-sarcoplasmic reticulum (SR) free $[Ca^{2+}]$ ($[Ca^{2+}]_{SR}$), SR Ca^{2+} load and Ca^{2+} release.
- $[Ca^{2+}]_{SR}$ changes during E-C coupling (Ca^{2+} scraps), Ca^{2+} sparks/blinks and Ca^{2+} waves.
- Spatiotemporal $[Ca^{2+}]_{SR}$ gradients constrain intra-SR Ca^{2+} diffusion models.
- Controversies about SR Ca^{2+} release activation, termination and wave propagation.

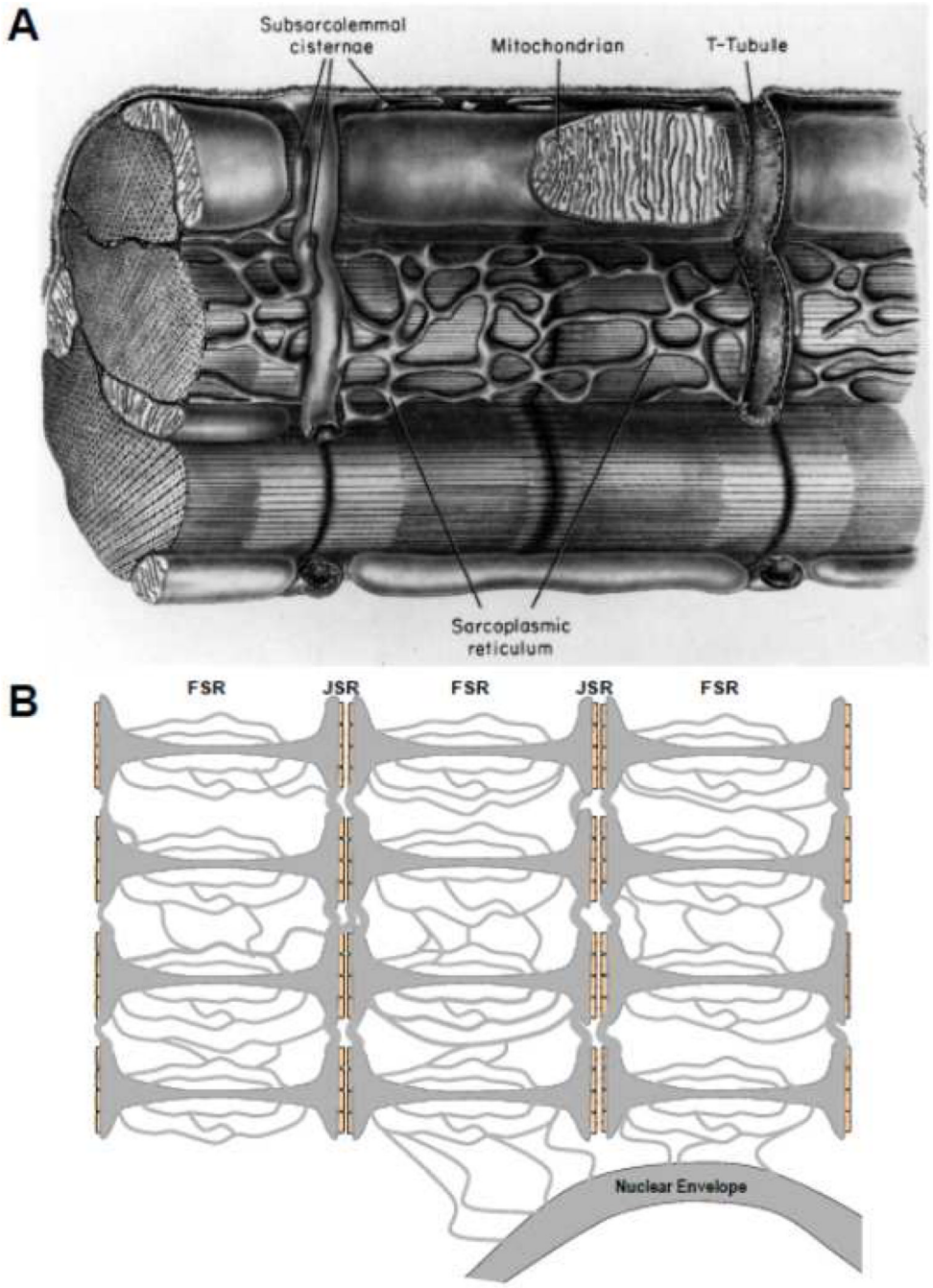

Figure 1.
Structure of SR in ventricular myocytes. A. Classic structural diagram reproduced from Fawcett and McNutt [32]. B. Schematic of FSR and JSR indicating longitudinal and transverse luminal connections, including to the nuclear envelope.

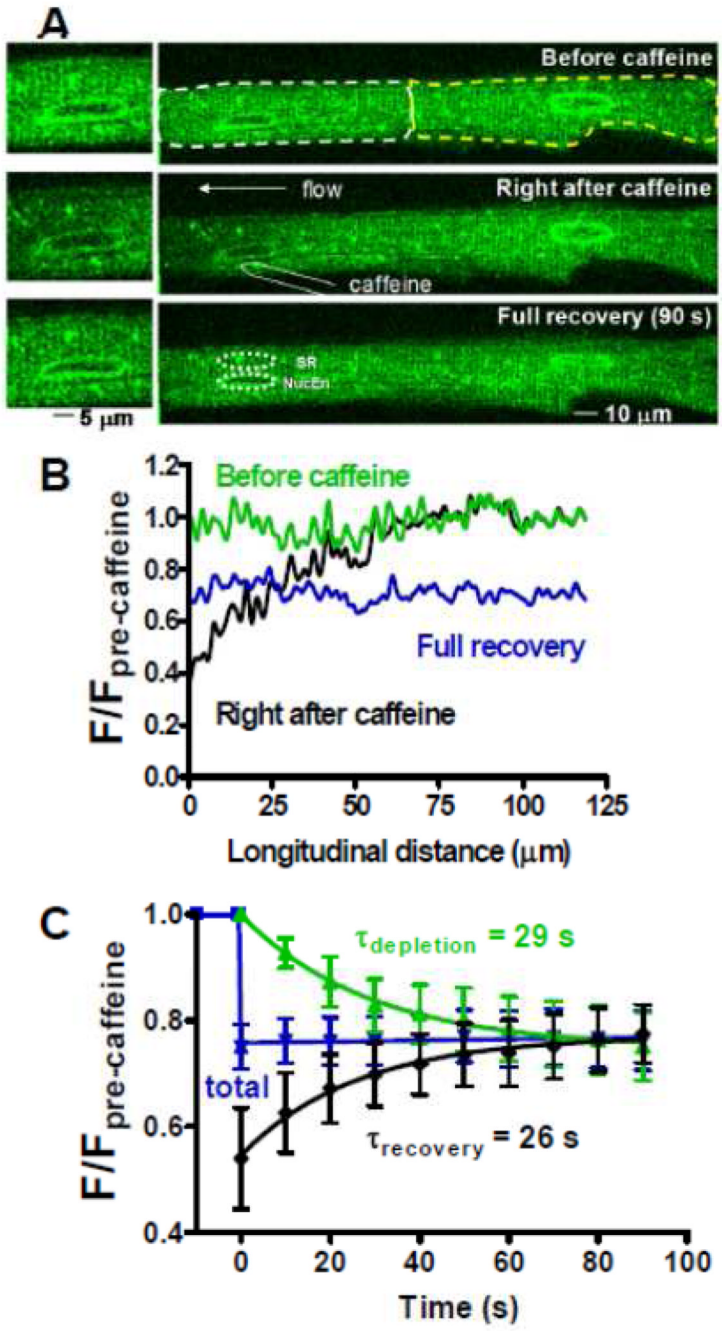

Figure 2.

Measuring Ca diffusion inside the SR. A. Fluo-5N signal before (top), immediately after (middle) a 1–2 s caffeine application to the left end of the cell and 90 s later (bottom; insets enlarge the region around the left nucleus). B. Longitudinal scans during these phases. C. Time-dependence of $[Ca]_{SR}$ signal from left (black), right (green) and whole (blue) cell. Modified from Wu and Bers [35] with permission.

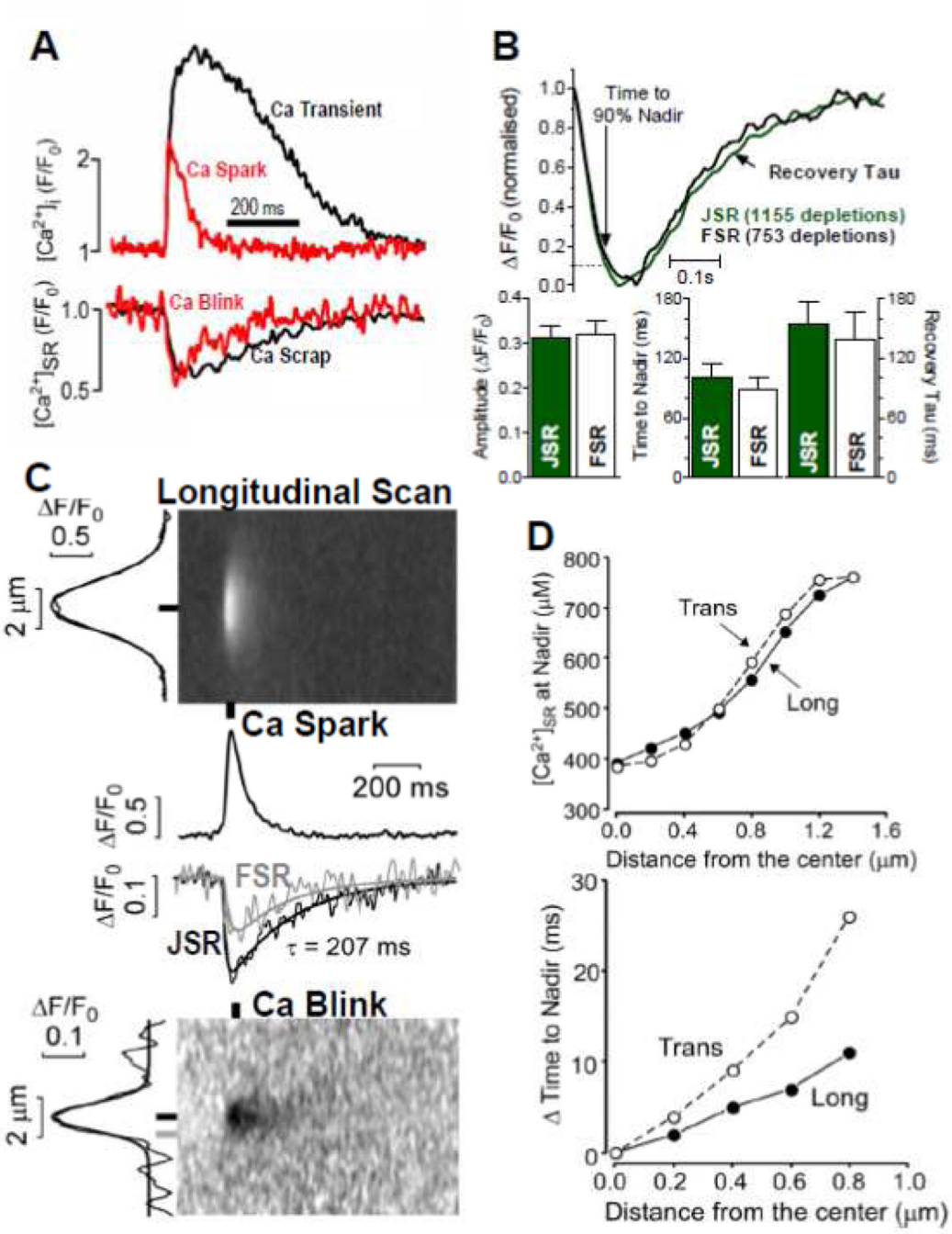

Figure 3.

Ca sparks and blinks with spatiotemporal resolution. A. Simultaneous measurements of a Ca transient and Ca scrap during ECC (black) and during a Ca spark and blink (modified from Zima *et al.* [24]. B. Kinetics and amplitude of Ca scraps measured at the Z-line (JSR) and mid sarcomere (FSR) showing average of indicated depletions and mean data in bar graphs. C. Simultaneous recordings of Ca spark and blink showing x-t images for longitudinal scans, time-dependent plots at the indicated locations and spatial width (at left edge) at indicated time. D. Distance-dependence going from Z-line to M-line of $[Ca]_{SR}$ and delay time for blink nadir (vs. that at the JSR). Averages of 37 traces. (B–D are modified from Picht *et al.* [25] with permission).

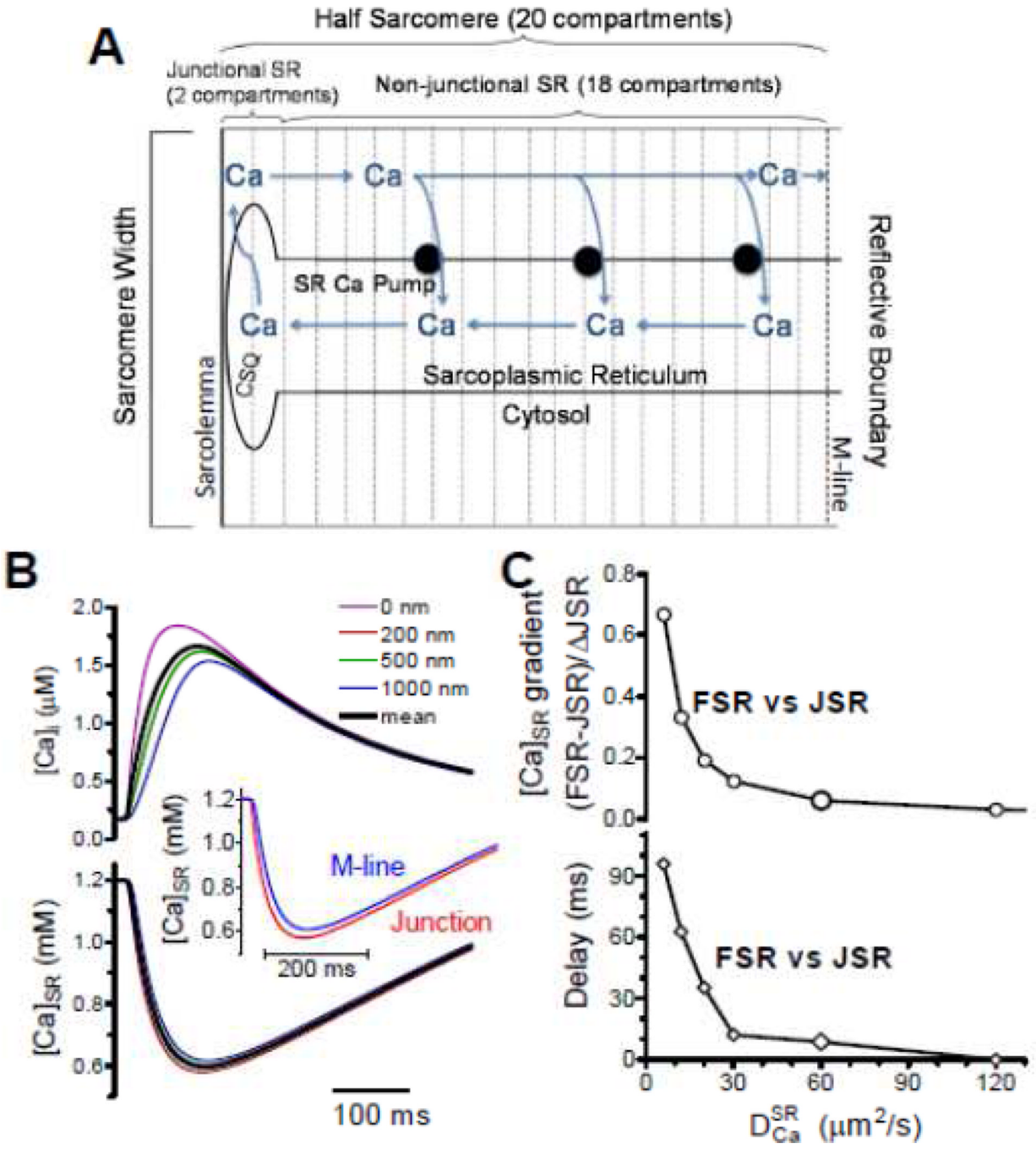

Figure 4.

Model of intra-SR diffusion during ECC. A. Structure and compartments of model. B. $[Ca]_i$ and $[Ca]_{SR}$ during a normal ECC-associated SR Ca release for D_{Ca}^{SR}=60 μm/s^2. C, D_{Ca}^{SR} – dependence of the $[Ca]_{SR}$ gradient and delay time for nadir between FSR and JSR (modified from Picht *et al.* [25] with permission).

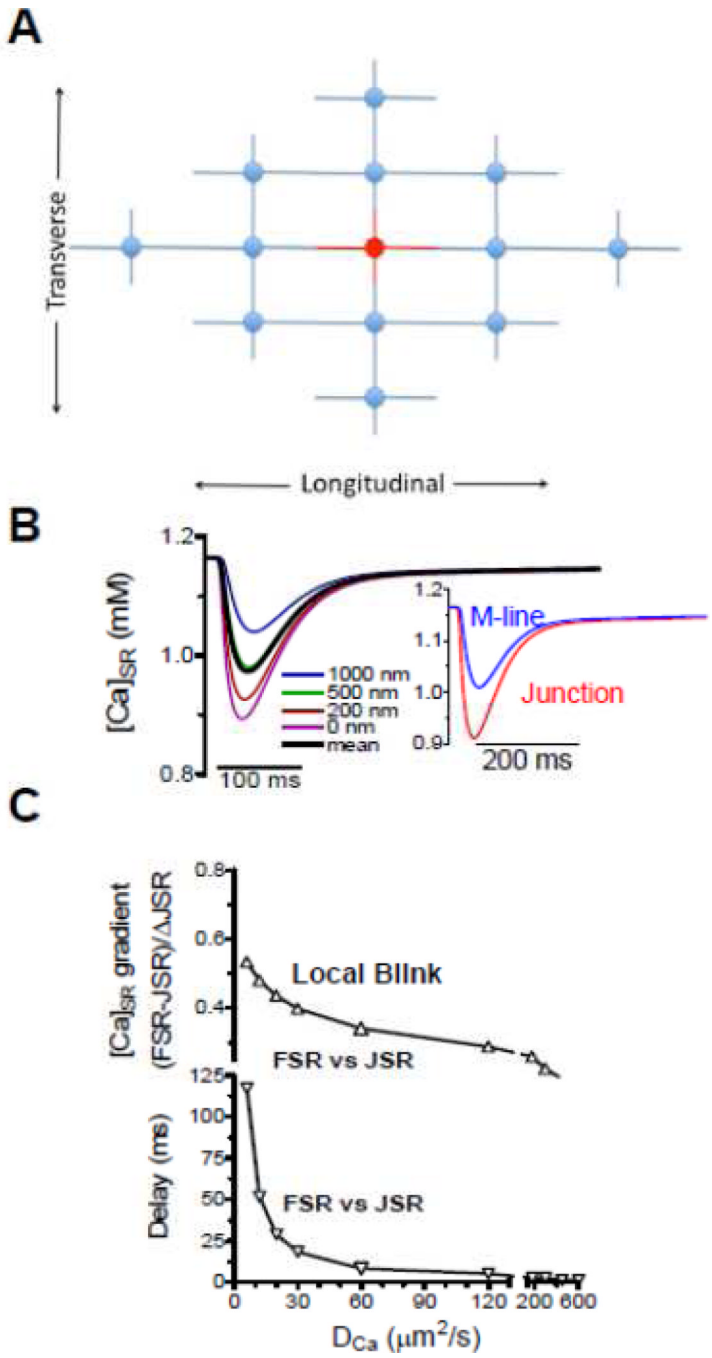

Figure 5.

Model of intra-SR diffusion during a Ca spark. A. Organization of junctions incorporated (not including above and below the plane). B. $[Ca]_{SR}$ during a normal ECC-associated SR Ca release for D_{Ca}^{SR}=60 μm/s^2. C. D_{Ca}^{SR} –dependence of the $[Ca]_{SR}$ gradient and delay time for nadir between FSR and JSR (modified from Picht *et al.* [25] with permission).

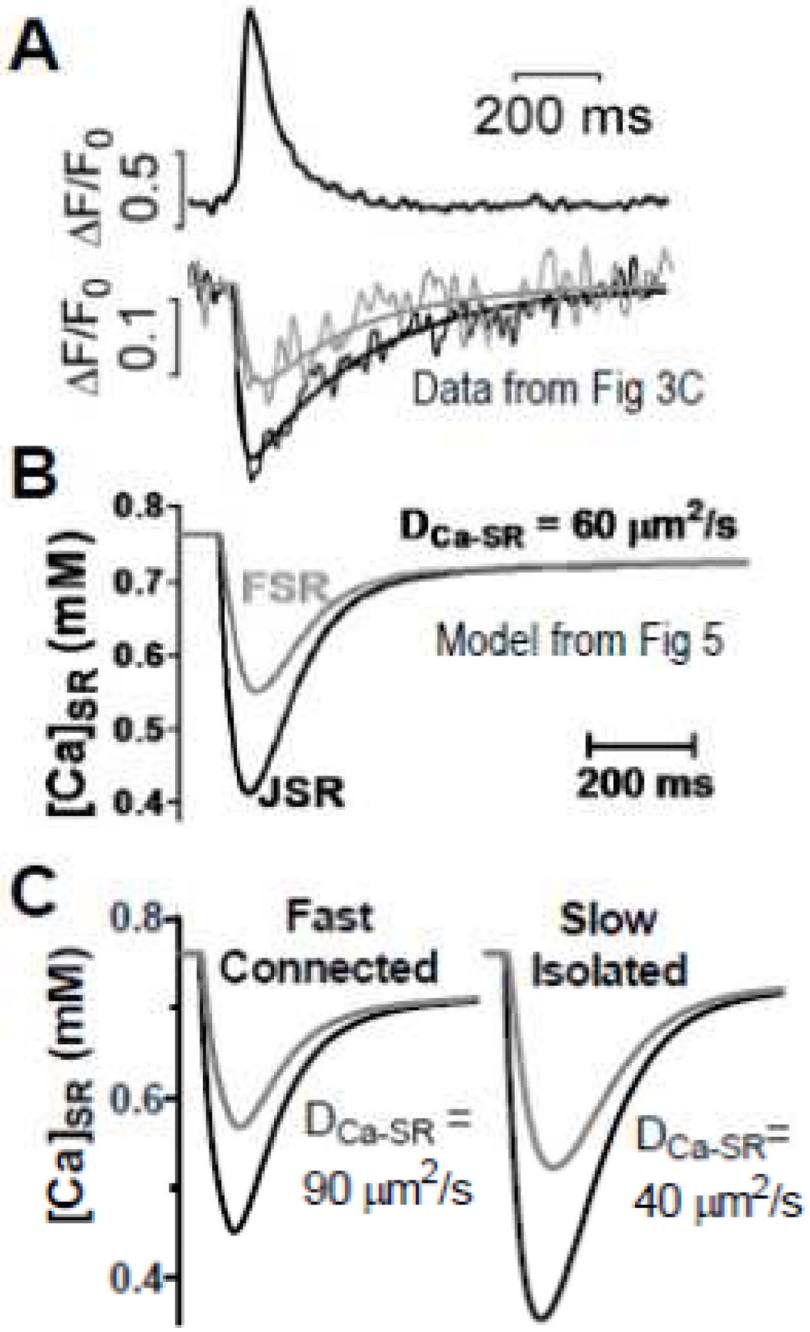

Figure 6.

$[Ca]_{SR}$ during Ca sparks. A–C. Curves are from experiments (A) and model (B) from [25]. C. Influence of fast/connected vs. slow/isolated junctions using altered D_{Ca}^{SR} (modified from Picht *et al.* [25] with permission).